

An ab Initio Study of S_N2 Reactivity at C6 in Hexopyranose Derivatives. I. Influence of Dipole–Dipole Interactions in the Transition Structure

Richard Dawes, Kathleen M. Gough,* and Philip G. Hultin*

Department of Chemistry, University of Manitoba, Winnipeg, Manitoba R3T 2N2, Canada

Received: October 30, 2003; In Final Form: August 4, 2004

It is widely accepted that dipole–dipole interactions in the S_N2 transition structure can play a dominant role in determining reaction rates. A model of this type was proposed some years ago to explain the remarkably low reactivity of galactopyranose-6-*O*-sulfonates toward S_N2 displacement, and similar arguments have recently been restated in the context of gas-phase reactions. In this paper, we present ab initio calculations (B3LYP/6-31+G(d,p)) on model structures and an analysis of charge densities using the theory of atoms in molecules. We find that the maximum possible impact of local dipole–dipole interactions is insufficient to account for the observed reactivity differences.

Introduction

The S_N2 displacement may appear to be among the simplest organic reactions, but recent experimental and theoretical investigations have revealed surprising aspects of this ubiquitous process.^{1,2} The availability of accurate computational methods has made it relatively straightforward to rigorously investigate anomalies in reactivity that had previously only been interpreted through qualitative descriptions. A striking example of such an anomaly comes from synthetic carbohydrate chemistry.

It has been known for many years that C6 sulfonate derivatives of hexopyranosides having the galacto configuration (i.e., C4–OR axial) display very low reactivities toward anionic nucleophiles, whereas the corresponding gluco-configured C6 sulfonates (C4–OR equatorial) react at rates typical of primary centers.³ In a rare example in which galacto- and gluco-compounds were subjected to a comparative kinetic study, the second-order rate constant for the reaction of azide with methyl-2,3,4-tri-*O*-acetyl-6-*O*-*p*-tolylsulfonfyl- α -D-glucopyranoside was observed to be 32-fold greater than that for the reaction of the analogous galactoside.⁴ In the majority of cases, attempted displacement of a C6 sulfonate from a galactopyranoside fails completely and instead leads to 5,6-elimination or to the formation of a 3,6-anhydrosugar in competition with the expected S_N2 product, which is obtained in very low yield.⁵ These examples are illustrative of cases in which the rates of S_N2 displacement apparently depend on the relative geometries of remote polar substituents.

In 1969, A. C. Richardson proposed a persuasive qualitative explanation for reactivity differences of this type.⁶ This rationalization assumed that differences in reactivity between the axial (galacto) and equatorial (gluco) configurations were a consequence of the differences in the energies of the respective transition structures. He argued that the transition structure for displacement would have a geometry in which the scissile C6–X bond was orthogonal to the C5–O5 bond, to minimize dipolar repulsion from interactions with the endocyclic oxygen. When O4 carried a bulky blocking group, the low reactivity of galacto-configured sulfonates was deemed to have a steric origin.

* Authors for correspondence. E-mail: hultin@cc.umanitoba.ca (P.G.H.); kmgough@ms.umanitoba.ca (K.M.G.).

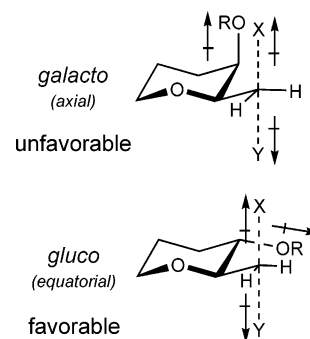


Figure 1. Postulated dipole interactions in S_N2 displacements at C6 in galactopyranosides.

In the absence of a bulky substituent on O4, he suggested that dipole–dipole interactions destabilized the S_N2 transition structure (Figure 1); more specifically, the developing negative charge on the leaving group X would encounter unfavorable dipolar interactions with an axial electronegative group at C4 (as in the galacto configuration). In the gluco configuration, the equatorial C4–OR group would not create this destabilizing effect. Richardson used a similar dipole rationalization to explain differences in the S_N2 reactivities of *O*-sulfonate derivatives of the secondary hydroxyl groups in hexopyranosides.

This steric/dipolar explanation has been nearly universally adopted by the carbohydrate community and is incorporated with very little comment into current textbooks.⁷ It continues to be extensively cited and has been applied outside carbohydrate chemistry.⁸ Craig and Brauman have recently restated a version of this rationale to explain rates of gas-phase S_N2 displacements in a series of *o*-substituted primary *n*-alkyl chlorides, although, in this case, they invoked favorable transition structure dipoles that *enhanced* reaction rates.⁹

Despite its intuitive appeal and the breadth of its applicability, the fundamental correctness of the steric/dipole model is not obvious; moreover, it has never been examined in the light of modern electronic theory. Although the initial description of the model only addressed reactions of sugars, it is apparent that the question of its validity has implications for understanding S_N2 reactivity in general. If the differences in S_N2 reaction rates are due to intramolecular dipole–dipole repulsions between the

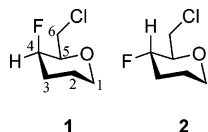


Figure 2. Tetrahydropyran model structures used in this study. Carbon atoms are designated using carbohydrate numbering.

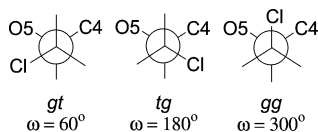


Figure 3. Newman projections of idealized C5–C6 rotamers (hydrogens omitted for clarity).

group at C4 and the leaving group at C6, we would expect to find structural distortions and local variations in charge density adopted to minimize these effects. Within the atoms-in-molecules (AIM) formalism, this would be partly manifested as an increase in the energies of the atoms in question. In our *ab initio* study of S_N2 identity displacements by chloride ion at the C6 positions in gluco- and galacto-configured model systems, we have examined the energetics of reactant rotamers as well as S_N2 transition structures. We have also performed detailed analyses of the charge densities of these structures within the theory of atoms in molecules and evaluated the possible magnitude of dipole–dipole interactions using a vector analysis approach.

Computational Models

The gluco- and galactopyranose systems under consideration have a tremendous number of available conformational minima when all possible rotations of the hydroxyl groups are considered. Tetrahydropyran model structures **1** and **2** (Figure 2) were chosen for our study. In these models, hydrogens replace the C1, C2, and C3 hydroxyl groups of the monosaccharides, while the C4 hydroxyl is replaced by fluorine. This is anticipated to maximize any potential dipole–dipole interaction. The steric environment at C6 in the simpler structures will not differ significantly from that in the actual monosaccharide derivatives, and the electronic effects most relevant to the S_N2 displacement at C6 are maintained. Furthermore, while most actual examples of these reactions have employed an aryl- or alkylsulfonate leaving group, we saw several advantages to using a halide identity reaction. First, there are many fewer degrees of freedom within the leaving group itself. Second, the local dipole effect is both simplified and accentuated in these structures. The identity reaction also avoids further complications involving differing electronegativities and steric factors. Chloride ion's electronegativity (3.0 Pauling, 3.02 Boyd¹⁰) is reasonably close to that of a methanesulfonate ester group (3.56, calculated using Boyd's method).

Electronic structure calculations were performed using parallel-enabled *Gaussian 98*,¹¹ as well as *Gaussian 98W*,¹¹ with topological charge density analyses conducted using AIM2000.¹² All energies and charge densities were calculated at the B3LYP/6-31+G(d,p) level of theory.¹³

The O5–C5–C6–Cl torsion (dihedral ω) defines three rotamers, conventionally identified as **gt**, **tg**, and **gg** (Figure 3). Initially, the C5–C6 rotamers of substrates **1** and **2** were identified in a series of geometry optimizations. To better characterize the C5–C6 rotational potential energy surface, the rotational transition structures connecting these minima were also obtained. By beginning from the rotational minima, transition structures and reaction coordinates for S_N2 displace-

TABLE 1: Calculated Dihedral Angles ω 's ($^\circ$) and Relative SCF Energies (kcal mol⁻¹) for Stationary Points in Galacto Model **1** and Gluco Model **2**

structure	ω	ESCF
1gt	70.9	1.024
TS _{1gt→1tg}	116.1	2.797
1tg	169.3	0.000
TS _{1tg→1gg}	248.8	7.673
1gg	301.2	5.026
TS _{1gg→1gt}	355.5	8.318
1TS		17.142 ^a
2gt	71.0	0.000
TS _{2gt→2tg}	128.2	2.740
2tg	157.6	2.317
TS _{2tg→2gg}	225.9	5.664
2gg	295.0	0.138
TS _{2gg→2gt}	360.6	6.457
2TS		10.568 ^a

^a Relative to lowest energy rotamer + chloride ion.

ments were located. Vibrational analysis verified the existence of one imaginary frequency for all transition structures and the lack of any imaginary frequencies for all minima.

To probe the potential role of dipole–dipole interactions in the transition structures, we performed topological analyses of the charge densities according to the theory of atoms in molecules.¹⁴ The full set of atomic properties for each atom was obtained from the previously calculated wavefunctions using the AIM2000 program.¹² To estimate the maximum possible classical dipole–dipole repulsion energy in the transition structures, local fragment dipoles and their interaction energies were calculated.

Because only subtle differences in atomic properties were anticipated throughout the various structures, our integration accuracy criteria were stringent. The atomic volume-integrated Laplacian of the charge density, defined as

$$L(\Omega) = -\frac{1}{4} \int_{\Omega} \nabla^2 \rho(\mathbf{r}) \, d\mathbf{r} \quad (1)$$

where Ω is an atomic basin, vanishes for an exact integration and can be considered as an error function for numerical integrations.¹⁵ Integrations were performed in natural coordinates with the β -sphere diameter set at the distance from the nucleus to the nearest critical point. Absolute and relative integration accuracies were set as low as 1×10^{-6} , and the integration path as large as 2.5×10^6 , as necessary to achieve a value for $L(\Omega)$ of less than 3×10^{-4} for heavy atoms and 1×10^{-4} for hydrogen. These criteria¹⁵ allow recovery of molecular self-consistent field (SCF) energies to within 0.2 kcal mol⁻¹, charges to within 2×10^{-3} e, and molecular dipoles to within 5×10^{-4} au. We note that the use of the AIM2000 default criteria results in sufficient accumulated error to misidentify the lowest-energy rotamer.

Results and Discussion

Rotameric Equilibria. Our gas-phase calculations located three rotational minima for each of **1** and **2**, corresponding to the expected staggered conformations. We also located the rotational transition structures between the rotamers. The calculated dihedral angles and energies for these structures are summarized in Table 1. In all cases, the rotational barriers were sufficiently low that the model systems would be in thermal equilibrium at the temperatures under consideration.

S_N2 Transition Structures. Transition structures (TSs) for the S_N2 displacements were sought beginning from each of the

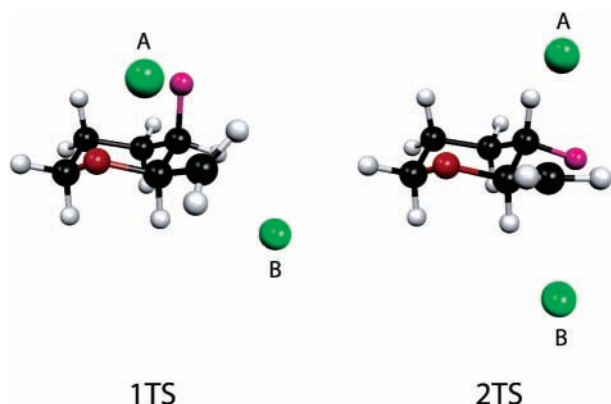


Figure 4. Transition structures for identity S_N2 displacements of **1** and **2**. Chlorines are arbitrarily designated as A or B for discussion purposes.

rotational minima of **1** and **2**. In each model system, only one viable nucleophile trajectory was found, leading to first-order saddle points (transition structures **1TS** and **2TS**, Figure 4) on the respective reaction energy surfaces. In the galacto system, transition structure **1TS** connects the **1gg** and **1tg** rotamers, while in the gluco system, transition structure **2TS** connects the **2gg** and **2gt** rotamers. For discussion purposes, we have labeled the Cl “above” the plane of the ring as Cl_A and the other as Cl_B.

The energy of the TS relative to the lowest-energy rotamer differs greatly between the two model compounds. Galacto transition structure **1TS** lies 17.14 kcal mol⁻¹ above **1tg**, whereas gluco transition structure **2TS** is only 10.57 kcal mol⁻¹ above **2gt** (Table 1), yielding an overall difference between the two systems of 6.57 kcal mol⁻¹, to be accounted for in some manner.

The orientation of the Cl_A–C6–Cl_B groups with respect to the ring systems at the transition structures depends strongly on the reactant C5–C6 rotational potentials. In the galacto case, **1tg** is the favored reactant rotamer, while **1gg** is disfavored. The S_N2 transition structure **1TS** has a torsion angle ω for Cl_A inclined considerably toward O5, such that ω for Cl_B is within 15° of that found in the low-energy **1tg** rotamer. Similarly, in gluco compound **2TS**, the **2tg** rotamer is disfavored, and the Cl_A–C6–Cl_B group twists toward the favorable **2gt** orientation. The Cl_A–C6–Cl_B angles deviate considerably from the idealized 180° values seen in symmetric methyl halide reactions; however, the deflection angles (~150°) are typical of calculated transition structures for identity S_N2 reactions involving chloride.¹⁶ We conclude that the calculated transition structures are not distorted to minimize repulsive interactions.

Atoms-in-Molecules Analysis. Some insight into experimental and predicted rates is provided by AIM analysis of energies, local dipole moments, and charge fluctuations for relevant fragments of the rotamers of **1** and **2** and in the S_N2 transition structures **1TS** and **2TS**. First, by partitioning a molecule into its constituent atoms, the energies of each atom can be compared through the various structures, revealing the changing relative contributions to the molecular energies. In this way, we can ascertain whether the chlorine and fluorine atoms in the galacto **1gg** rotamer are perturbing each other relative to the lower-energy rotamers and whether there is greater perturbation in galacto **1TS** than in gluco **2TS**. Second, we can calculate local distortions of the charge densities. If the dipole model were correct, then rotation at C6 from a low-energy rotamer into the disfavored position would induce opposing dipoles into both molecular fragments. Likewise, a greater induced dipole would be expected in **1TS** than in **2TS**.

TABLE 2: Selected AIM Atomic Charges (e) for Reactant Rotamers and S_N2 Transition Structures

atom	1gt	1tg	1gg	1TS	2gt	2tg	2gg	2TS
C1	0.525	0.519	0.524	0.539	0.525	0.519	0.524	0.526
C2	0.079	0.080	0.079	0.077	0.075	0.076	0.075	0.076
C3	0.082	0.082	0.081	0.080	0.083	0.081	0.083	0.081
C4	0.506	0.504	0.528	0.511	0.510	0.527	0.510	0.506
C5	0.563	0.554	0.567	0.561	0.558	0.544	0.558	0.549
C6	0.158	0.153	0.161	0.107	0.149	0.155	0.151	0.095
O5	-1.053	-1.054	-1.054	-1.025	-1.058	-1.056	-1.058	-1.041
Cl _A	-0.263	-0.276	-0.235	-0.654	-0.262	-0.253	-0.265	-0.709
F4	-0.640	-0.639	-0.638	-0.642	-0.643	-0.639	-0.642	-0.643
H6R	0.069	0.049	0.026	0.121	0.043	0.054	0.052	0.134
H6S	0.029	0.067	0.042	0.112	0.056	0.033	0.047	0.139
Cl _B				-0.677				-0.675

TABLE 3: Differences in AIM Atomic Energies (kcal mol⁻¹) and Charges (e) Relative to Low-Energy Rotamers

	1gt	1gg ^a	2tg ^a	2gg
	Δenergy (Δcharge)		energy (Δcharge)	
F	-2.04 (-0.001)	-7.24 (0.001)	-1.46 (0.003)	2.22 (0.001)
C4	2.45 (0.002)	11.83 (0.024)	5.94 (0.017)	-3.20 (0.000)
C5	3.25 (0.008)	8.77 (0.012)	-0.71 (-0.015)	1.53 (-0.001)
C6	2.93 (0.004)	10.65 (0.008)	5.11 (0.006)	2.31 (0.002)
Cl	3.88 (0.012)	6.54 (0.040)	-1.75 (0.009)	-2.41 (-0.002)
O	-5.04 (0.001)	-5.62 (0.000)	5.13 (0.003)	-0.85 (0.000)

^a High-energy rotamer. For **1**, energies and charges are relative to **1tg**; for **2**, relative to **2gt**.

The net atomic charges in the reactant rotamers and the S_N2 transition structures were computed through AIM (Table 2); atomic charges on ring hydrogens are less than 0.03 e (not shown). The atomic charges change by, at most, a few hundredths of an electron through the C5–C6 torsional rotamers in both **1** and **2**. Note that the additional negative charges in **1TS** and **2TS** remain largely localized on the chlorines. The C6 becomes markedly less positive, while the two hydrogens take on a significantly more positive character. This is consistent with the reported results for other identity S_N2 reactions.^{16b} There is no evidence for any destabilizing electrostatic effects in the charge distributions in the **1gg** and **2gt** rotamers or the transition states.

In contrast, the AIM energies of the various atoms exhibit relatively large changes among the rotamers (Table 3). Because the summed molecular energies differ by about 5 kcal mol⁻¹ at most, it might be surprising that many individual atomic energies vary by more than twice that. Moreover, the AIM atomic energies do not change in a manner consistent with direct destabilizing electrostatic interactions. In the galacto compound, upon going from the preferred **1tg** to the high-energy **1gg** rotamer, the chlorine energy rises but the fluorine energy drops. In the gluco compound, both the fluorine and chlorine atoms in the high-energy **2tg** rotamer are lower in energy than they are in the lowest-energy **2gt** rotamer. Furthermore, the summed system energy changes cannot be recovered from the changes in a few key atoms. Energy is redistributed throughout the molecule, including hydrogens and more remote heavy atoms. Some patterns in the energy fluctuations point to complex long-range interactions. For example, the ring oxygen is destabilized by ~5 kcal in both **1** and **2** when the chlorine atom is trans to it. These interactions present an interesting direction for future investigation.

In both **1** and **2**, the disfavored rotamers are those in which the C6–Cl bond is aligned with the C4–F bond (Table 1); in the galacto case, the **1gg** rotamer lies 5.026 kcal mol⁻¹ above minimum; in the gluco case, the **2tg** rotamer is 2.32 kcal mol⁻¹ above the minimum. It might be argued that this too is evidence

TABLE 4: Orientation and Magnitude of the C4–F Atomic Dipole in Rotamers and Transition Structures

structure	C5–C4–F– μ ($^\circ$) ^a	C4–F– μ ($^\circ$) ^b	$ \mu(\text{F}) $ (D)
1gt	165.7	136.4	0.32
1tg	172.4	143.7	0.31
1gg	164.1	128.9	0.36
1TS	–169.5	14.2	0.30
2gt	–176.6	151.6	0.32
2tg	–179.3	155.3	0.56
2gg	162.3	158.1	0.32
2TS	110.6	11.7	0.30

^a Dihedral angle of dipole vector $\mu(\text{F})$ with C5–C6–F bond path.

^b Angle of dipole vector $\mu(\text{F})$ with C4–F bond.

of a repulsive dipolar interaction. Within the AIM formalism, each atom has an atomic dipole representing asymmetry of charge within its defined atomic basin. The molecular dipole is found from the summed contributions from the atomic dipoles and the relative positions of the charged nuclear attractors. We have examined the atomic dipoles at F for all six rotamers and the two transition structures (Table 4).

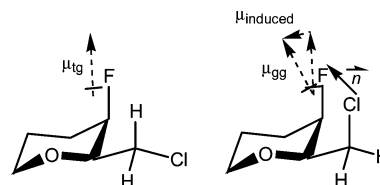
Changes in the orientation and magnitude of $\mu(\text{F})$ were barely perceptible throughout the ground-state rotamers. The magnitudes and orientations of the individual atomic dipoles did not display any pattern consistent with a repulsive dipolar interaction in the reactant rotamers. The dipoles at F and Cl (data not shown) are directed outward, away from the ring and roughly away from O5.

In both **1TS** and **2TS**, the orientations of $\mu(\text{F})$ are radically different from their counterparts in the rotamers, being nearly aligned with the C–F bond. Similarly, $\mu(\text{Cl}_A)$ in the transition structures is roughly collinear with the $\text{Cl}_A\text{--C6--Cl}_B$ axis. We therefore attempted to evaluate potential dipole–dipole interactions between these fragments.

The experimental galacto/glucos relative rates of 0.03–0.05, determined by Wu et al.,⁴ indicate that the faster glucos reaction is favored by 2.9–2.5 kcal mol^{–1}. In many cases mentioned in the synthetic literature, the relative galacto rates must have been much smaller than this, because the galacto product could not be isolated in any appreciable yield even after extended reaction times.⁷ In our model systems, the difference in relative energies is over 6.5 kcal mol^{–1}. At the distance between the C4–F and C6–Cl bond critical points in **1TS** (3.08 Å), two dipoles of 3.65 D in perfect alignment would be needed to account for this energy difference. While it is only a very rough approximation, we modeled Richardson’s local fragment dipoles from the AIM properties of C4 and F, and C6 and Cl, relative to the bond critical points between them. From the calculated local moments, classical dipole–dipole interaction energies were obtained. The difference in the C4–F/C6–Cl_A dipole–dipole interaction energies in **1TS** and **2TS** was only 1.84 kcal mol^{–1}, which is less than one-third of our calculated energy difference. In **1TS** where some solvent penetration would be expected, any interaction energies due to dipoles would be further reduced. Once again, it appears unlikely that this type of interaction could explain a substantial portion of the S_N2 reactivity differences.

Finally, to monitor changes in the local C4–F dipole as a function of the orientation of the chloromethyl group, any induced atomic dipole at F or C4 was projected onto a vector \bar{n} in the direction of the supposedly perturbing chlorine atom (Figure 5).

The projections of the induced dipoles onto the normalized $\text{Cl}_A \rightarrow \text{F}$ vectors (Table 5) contain contributions from differences in charge transfer and in atomic dipoles (C4 and F), relative to those of the lowest-energy rotamer.¹⁷ There is very little

**Figure 5.** Possible induced atomic dipoles arising from conformational change.**TABLE 5: Projection of Induced Dipoles^a (au) onto Normalized $\text{Cl}_A \rightarrow \text{F}$ Vectors \bar{n}**

atom	1gt	1gg	1TS	2tg	2gg	2TS
F	–0.003	0.025	0.041	0.031	0.004	0.024
C4	–0.019	0.069	0.088	0.106	0.030	–0.007

^a Induced atomic dipoles relative to the low energy rotamers **1gt** and **2gt**.

difference in atomic charges on C4 and F among the reactant rotamers (Table 2), and the calculated fragment dipole is directed precisely along the C4–F bond, which is nearly orthogonal to the $\text{Cl}_A \rightarrow \text{F}$ vector. Thus, the dominant contributions to the induced dipole are from changes in atomic dipoles, which are very small in all cases.

Summary

Analysis of the S_N2 transition structures revealed no significant structural perturbations that may be ascribed to dipole–dipole repulsion. The complete set of AIM-derived properties, including atomic energies, charges, and dipoles, revealed no correlation with the putative dipolar repulsion in these transition structures. Estimates of the maximum energy attributable to dipole–dipole interactions in the transition structures showed that such interactions can make only minor contributions to the S_N2 reactivity differences between glucos and galacto systems at C6. AIM analysis of the reactants likewise indicated that differences in rotameric energies could not be attributed to dipole–dipole interactions between the F and Cl.

The AIM analysis did reveal small changes in atomic properties throughout the molecular structures in the various rotamers and in the S_N2 transition structures that point toward the possibility of a rich scheme of influences even from somewhat remote sites. In the companion paper, we describe an extension of this work to two additional pairs of model systems. The role of reactant populations, including solvation, is explored. A complete free-energy and kinetic analysis is included. We present analysis of the intrinsic reaction coordinate (IRC) paths and their curvature that provides valuable insight into these S_N2 processes.

Acknowledgment. This work was funded by Natural Sciences and Engineering Council of Canada Research Grants to K.M.G. and P.G.H. Richard Dawes received a scholarship from Medicare, Inc. We thank Dr. Richard Bader and Mr. Chérif Matta (McMaster University), Dr. Tom Ziegler (University of Calgary), and Dr. Bob Wallace (University of Manitoba) for helpful discussions. The authors acknowledge the use of the University of Manitoba High Performance Computing Facilities (<http://www.umanitoba.ca/campus/acn/hpc/>). P.G.H. also thanks Dr. Walter A. Szarek (Queen’s University) for suggesting the steric/dipole model to explain an unexpected result many years ago.

Supporting Information Available: Coordinates and absolute energies for all stationary points; table of AIM atomic

energies, dipoles, and charges for **1**, **2**, **1TS**, and **2TS**; details of vector analyses. This material is available free of charge via the Internet at <http://pubs.acs.org>.

References and Notes

- (1) Hase, W. L.; Sun, L.; Song, K. *Science* **2002**, *296*, 875.
- (2) Regan, C. K.; Craig, S. L.; Brauman, J. I. *Science* **2002**, *295*, 2245–2247.
- (3) Ball, D. H.; Parrish, F. W. *Adv. Carbohydr. Chem. Biochem.* **1969**, *24*, 139–197.
- (4) Wu, M.-C.; Anderson, L.; Slife, C. W.; Jensen, L. J. *J. Org. Chem.* **1974**, *39*, 3014–3020.
- (5) (a) Mulard, L. A.; Kovác, P.; Gludemans, C. P. J. *Carbohydr. Res.* **1994**, *259*, 117–119. (b) Ali, M. A.; Hough, L.; Richardson, A. C. *Carbohydr. Res.* **1991**, *216*, 271–287.
- (6) Richardson, A. C. *Carbohydr. Res.* **1969**, *10*, 395–402.
- (7) Collins, P. M.; Ferrier, R. J. *Monosaccharides. Their Chemistry and Their Roles in Natural Products*; Wiley: Chichester, 1995.
- (8) Seebach, D.; Chow, H.-F.; Jackson, R. F. W.; Sutter, M. A.; Thaisrivongs, S.; Zimmermann, J. *Liebigs Ann. Chem.* **1986**, 1281–1308.
- (9) Craig, S. L.; Brauman, J. I. *J. Am. Chem. Soc.*, **1999**, *121*, 6690–6699.
- (10) Boyd, R. J.; Boyd, S. L. *J. Am. Chem. Soc.* **1992**, *114*, 1652–1655.
- (11) Frisch, M. J.; Trucks, G. W.; Schlegel, H. B.; Scuseria, G. E.; Robb, M. A.; Cheeseman, J. R.; Zakrzewski, V. G.; Montgomery, J. A.; Stratmann, R. E.; Burant, J. C.; Dapprich, S.; Millam, J. M.; Daniels, A. D.; Kudin, K. N.; Strain, M. C.; Farkas, O.; Tomasi, J.; Barone, V.; Cossi, M.; Cammi, R.; Mennucci, B.; Pomelli, C.; Adamo, C.; Clifford, S.; Ochterski, J.; Petersson, G. A.; Ayala, P. Y.; Cui, Q.; Morokuma, K.; Malick, D. K.; Rabuck, A. D.; Raghavachari, K.; Foresman, J. B.; Cioslowski, J.; Ortiz, J. V.; Stefanov, B. B.; Liu, G.; Liashenko, A.; Piskorz, P.; Komaromi, I.; Gomperts, R.; Martin, R. L.; Fox, D. J.; Keith, T.; Al-Laham, M. A.; Peng, C. Y.; Nanayakkara, A.; Gonzalez, C.; Challacombe, M.; Gill, P. M. W.; Johnson, B. G.; Chen, W.; Wong, M. W.; Andres, J. L.; Head-Gordon, M.; Replogle, E. S.; Pople, J. A. *Gaussian 98W*, Revision A.7 or A.11parallel; Gaussian, Inc.: Pittsburgh, PA, 1998.
- (12) Biegler-König, F.; Schönbohm, J.; Bayles, D. *J. Comput. Chem.* **2001**, *22*, 545–559.
- (13) (a) Becke, A. D. *J. Chem. Phys.* **1993**, *98*, 5648–5652. (b) Stephens, P. J.; Devlin, F. J.; Chabalowski, C. F.; Frisch, M. J. *J. Phys. Chem.* **1994**, *98*, 11623–11627.
- (14) Bader, R. F. W. *Atoms in Molecules: a Quantum Theory*; The International Series of Monographs on Chemistry 22; Clarendon Press: Oxford, 1990.
- (15) Aicken, F. M.; Popelier, P. L. A. *Can. J. Chem.* **2000**, *78*, 415–426.
- (16) (a) Lee, I.; Kim, C. K.; Chung, D. S.; Lee, B.-S. *J. Org. Chem.* **1994**, *59*, 4490–4494. (b) Streitwieser, A.; Choy, G. S.-C.; Abu-Hasanayn, F. *J. Am. Chem. Soc.* **1997**, *119*, 5013–5019.
- (17) In the AIM formalism, although the total molecular energy is recovered by summing the atomic contributions, the recovery of molecular dipoles is less straightforward. Because the charge is partitioned into atomic basins, each “atom” has a net charge (summing to zero for a neutral molecule) and an atomic dipole representing asymmetry of charge within the atomic basin. To recover a molecular dipole from atomic charges and dipoles, the contribution from the relative positions of the charged nuclear attractors is added to that of the sum of the atomic dipoles (ref 14). When a dipole is induced by a perturbation such as an applied field, or as in our case the change of conformation, there are two possible contributions. The atomic dipoles representing distortion of charge within the basins change. There is also a change in the charge-separation term that includes transfer of charge across the interatomic boundary, changing the amount of charge being separated, and geometry relaxations that change the distance by which charge is separated. The charge-separation contribution to the dipole is directed precisely between the two nuclear attractors, while in general, the atomic dipole contribution can be in any direction.